

## Architecture Level Resource Optimization of Orbital Parameters, Propulsion Solutions, and Power Transmission Frequency for Space Solar Power System in Low Earth Orbit

Mark Dunn\*\*, Peyton Burlington\*\*, Abdulbari Agboola\*\*

<sup>a</sup> Department of Aerospace Engineering and Engineering Mechanics, University of Texas at Austin, 2617 Wichita St North Office Building A, Austin, TX 78712

\* Corresponding Author

### Abstract

This manuscript aims to identify the feasibility of a LEO Solar Power Satellite by hypothesizing its most economical altitude, eccentricity, inclination, and propulsion system subject to several non-deterministic physical models. Several design trade-offs were quantified in calculating the orbital altitude for maximum return on investment. This was done with physical models for gas dynamic drag, J2 perturbations, spacecraft heating, and atmospheric attenuation and space losses impacting wireless power transmission as a function of altitude. In this sense, the goal is to develop a theoretical database to study the trade-offs between different orbital configurations for an SPS. Several of these models are non-deterministic and require a level of Monte-Carlo analysis. Additionally, electric propulsion was identified as a good candidate for the primary propulsion system due to its high efficiency, long lifetime, and appropriate thrust levels for the hypothesized flight envelope. Within the regime of analysis, the preliminary orbital elements for the maximum economic efficiency of an SPS system of 25 sq. m frontal area feature a circular low-Earth orbit of altitude 404 km and an inclination of 63.4 deg, sustained by an electric propulsion system with thrust on the order of micronewtons. Ultimately, these models could be used to quantify the feasibility and reliability of an SPS system in LEO or aid in the advanced-stage development or design of a space-based solar power system.

**Keywords:** Solar Power Satellite, Low Earth Orbit, Optimization, Electric Propulsion, Physical Models

### Nomenclature

#### Variables:

$\alpha$ , thermal accommodation coefficient  
 $\beta$ , ratio of specular to diffuse molecular collisions with spacecraft wall  
 $\rho$ , atmospheric density  
 $d$ , distance  
 $f$ , frequency  
 $c$ , speed of light  
 $\lambda$ , wavelength  
 $\eta$ , efficiency  
 $A$ , antenna aperture area  
 $\omega$ , rotational speed  
 $\sigma$ , Stefan-Boltzmann constant  
 $\epsilon$ , surface emissivity  
 $C_D$ , coefficient of drag  
 $D$ , gas-dynamic drag  
 $V$ , spacecraft speed  
 $S$ , spacecraft area normal to gas flow

#### Suffixes:

p, propellant tank  
w, spacecraft wall  
E, Earth  
T, Thrust  
 $T_{\text{Resultant}}$ , Resultant Thrust  
 $\sigma_{\text{allow}}$ , allowable stress  
 $P_r$ , Power Received  
 $G_{\text{dB}}$ , Gain  
 $P_t$ , Power Transmitted  
 $G_t$ , Gain Transmitter  
 $G_r$ , Gain Receiver  
 $L_{\text{FSPL}}$ , Free Space Path Loss  
 $L_{\text{Atmospheric}}$ , Atmospheric Attenuation  
 $T_w$ , Thermal Wall Heating of Spacecraft

### Acronyms/Abbreviations

SSPS - Space Solar Power Satellite  
SPS - Space Power Satellite

WPT - Wireless Power Transmission  
TRL - Technology Readiness Level  
ABEP - Air-Breathing Electric Propulsion  
FSPL - Free Space Path Loss  
ITU - International Telecommunications Union  
FCC - Federal Communications Commission  
LEO - Low-Earth Orbit  
GEO - Geo-Stationary Orbit  
RGT - Repeating Ground Tracks  
PDF - Probability Distribution Function  
USD - United States Dollar

## 1. Introduction

Space-based solar power is a promising source of renewable energy, considered technically feasible since the 1970s [1]. There have been many crowds of support of this technology globally, spanning governments, research labs, and companies to prove the technology to be viable and economically feasible. The idea of space solar technology is to place solar acquisition devices in orbit to bypass the roughly 30% attenuation of incident solar radiation by Earth's atmosphere [2] and then distribute the power down to an Earth ground station via wireless power transmission. Up until January 2023 a solar power satellite (SPS) had never been demonstrated. This limited availability of experimental data and given the fact that many of its initial conceptual designs place the system in geostationary orbit (GEO) – a reasonable assumption is that there is not much data on the performance parameters of a low Earth orbiting (LEO) SPS as a function of its orbital elements. The initial conceptual designs focused on feasibility analyses of a system in GEO poses multiple benefits to the space-based solar power mission architecture; for instance, its 'frozen' ground tracks enable continuous power transmission from orbit to ground, while its high altitude (~35,786 km) minimizes Earth-induced eclipse times, maximizing solar energy acquisition periods. However, 'Earth-to-orbit transportation' remains one of the most costly aspects of such a campaign [2]. Many early conceptual designs [3] present massive structures with individual component sizes on the order of kilometers; the price-tag for a project of this scale is on the order of hundreds of billions of dollars, or, of the same order as the yearly military investment in the U.S.. While economically impractical, these designs are considered technically feasible assuming sufficient technological development in areas related to the in-space assembly of large structures and the development of high-efficiency solar energy conversion systems [1].

To ease economic prerequisites, recent feasibility studies and conceptual designs have shifted their focus to placement in low-Earth-orbit (LEO). Similarly, there has been an increased interest in modular architectures

that will allow the cumulative construction of a large-scale space solar power system [3]. Moreover, the present project focuses on enhancing economic efficiency via careful selection of the system's orbit, power transmission frequency, and propulsion system. As such, the project assumes that sufficiently advanced in-space assembly and photovoltaic technologies exist. This is a reasonable assumption given the high technology readiness level of most relevant technologies [4]. Thus, the information provided herein is of use to prospective advanced-stage development and not early design or technology viability assessments.

This project explores the economic merit of different orbital configurations, power transmission frequencies, and propulsion solutions by analytical methods, computational tools, and literature review. In particular, an orbital altitude and eccentricity Monte Carlo scheme is used to find the cost-optimal orbit for a space-based solar power system of varying size. Once an altitude is chosen, another Monte Carlo analysis is performed to quantify the variability of gas dynamic drag due to non-deterministic effects resulting from solar cycles and weather patterns. This variability then drives the requirements for the propulsion system.

Before determining the most cost-effective LEO orbit, a cost-optimized Power Transmission Frequency needs to be identified. Previous studies have investigated a range of frequencies, including 2 to 2.5 GHz, 5.87 GHz, and 35 GHz, with the latest research demonstrating terrestrial feasibility at 10 GHz [5, 6]. However, pinpointing a singular cost-optimal frequency still remains a question, influenced by the balance between low transmission losses and large required aperture size for low frequencies and vice versa for high frequencies. However, this study aims to identify this optimal frequency and then utilize it to optimize the orbital altitude based on the tradeoffs of free space path loss, which increases with altitude, and drag, which decreases with altitude.

Given our considerations that there is an optimal altitude to balance the effects of signal attenuation and power generation while under the effects of gas dynamic drag and other non-deterministic variables, methods of maintaining such an altitude have been analyzed to theoretically select a potential satellite propulsion system.

An area of interest to the study was ideal propulsion systems that could reliably station keep a prescribed LEO (100 km- 2000 km) given that gas dynamic drag would have a considerable effect on its performance. Given that there are various parameters of propulsion systems to take into account, our study consisted of analyzing propulsion and attitude control thrusting systems of various technology readiness levels (TRLs) as well as varying methods of propulsion, such

as electric and chemical engines. During initial literature reviews and optimization modeling, the altitude range was considered to be reasonably low (100 km- 400 km), therefore typical spacecraft engines such as ion and hall thruster electric engines were considered in our database, as well as air-breathing propulsion engines given their operating range up to 300 km [7, 8]. As our range of analysis increased, the engine considerations widened into other categories of engines with chemical propellants. To theoretically determine the optimal engine given a prescribed altitude, a qualitative and quantitative method of analysis was used given the engine parameters, i.e., weight, thrust, ISP, altitude of operation, and thrust-to-power Ratio. Each parameter was weighted, given the importance of each parameter to the satellite’s initial launch cost and lifetime operation.

## 2. Methodology

### 2.1 Wireless Power Transmission Frequency Analysis

The cost of the WPT losses due to an increased orbital altitude was quantified using a multi-step process. The first step is to identify the optimal frequency to minimize transmission losses. Then, calculate the transmission losses at that frequency and convert them to an economic factor as a function of orbital altitude, which will then be incorporated in the final tradeoff analysis. This multi-step process was analyzed and conducted using MATLAB.

### 2.2 Monte Carlo Analysis for Orbital Optimization

Two Monte Carlo analyses were performed throughout the present project. The first combined all of the presented relationships between performance parameters and orbital elements (e.g., drag as a function of altitude and launch cost as a function of eccentricity) by summing the estimated economic cost for each term. This was done for 15,000 different configurations of altitude and eccentricity. The configuration of minimum total economic cost is taken as that of highest economic merit. This optimization process was carried out for three different values of spacecraft frontal area: 5 sq. m, 25 sq. m, and 125 sq. m.

Once the configuration of highest economic merit was determined, a Monte Carlo analysis of the space environment relevant to that orbit was performed. The analysis used empirical data about atmospheric temperature and density to predict the fluctuation in drag and spacecraft heating that the solar power satellite may see throughout its operational lifetime. The empirical data was used to create probability distribution functions. The variance and range of these

functions is seen to be highly reflective of cycles in solar activity. However, due to the limited availability of atmospheric temperature data, a triangular distribution function is assumed with maximum and minimum values based on extrema in solar activity over a full cycle. The results from this space environment Monte Carlo could help guide the design of the space solar power’s propulsion and thermal management system.

### 2.3 Feasibility Assessment of Propulsion Solutions

To develop the basis of decisions to assess different propulsion systems a trade study was conducted of varying spacecraft engines and typical engineering decision choices were included in our initial study. Engineering design choices such as the engine fuel type, input/output power, the maximum recorded thrust, empty engine mass, engine efficiency, Isp, propellant thermodynamic parameters, altitude, and thrust-to-power Ratio were noted for each engine. The final assessment is limited to variables that varied widely across selections as described in **Appendix A**, such as the Thrust-to-Power Ratio, Altitude, Thrust, Isp, and Weight. A weighted decision matrix was used to select an optimal engine with a subjective weighting that valued long-term operation of the satellite over variables that are indicative of initial launch costs since the returns in value of the satellite is realized throughout the entire duration. The only variable that is optimized is the altitude variable which is the optimal altitude given the modeled drag force and recorded max thrust of the engine.

Table 1: Statistical Weighting of Propulsion Decision Analysis

Variable [Statistical Weight]	T/P Ratio * [x2]	Thrust** (Newtons) [x3]	Weight (kgs) [x2]	Altitude (km) [x1]	Isp (seconds) [x2]
4	> 6	> 6	0 to 1	<100	> 3000
3	4 to 6	3 to 6	2 to 5	100 to 500	2001 to 3000
2	1 to 3	1 to 4	6 to 9	501 to 1100	1000 to 2000
1	< 1	< 1	> 10	>1100	< 1000

\*Values on order of E-5

\*\*Values on order of E-1

## 3. Theory and calculation

The following section details the calculations and models resulting from our methodology of optimizing the transmission frequency, orbital altitude, and inclination.

### 3.1 Transmission Frequency Analysis

Three primary equations/models were used to identify the cost-optimal power transmission frequency. The Free Space Path Loss (FSPL), receiver gain, and the atmospheric attenuation. Atmospheric attenuation is modeled using the International Telecommunication Union's ITU-R P.676-10 [9]. FSPL is calculated using equation (1).

$$L_{FSPL} = 20\log_{10}(d) + 20\log_{10}(f) + 20\log_{10}\left(\frac{4\pi}{c}\right) \quad (1)$$

In addition, tradeoffs based on receiver effective aperture size were also considered. The antenna gain formula, which is a function of aperture area is shown below in (2)

$$G_{db} = 10\log_{10}\left(\frac{4\pi A}{\lambda^2}\right) \quad (2)$$

Finally all of the losses, antenna gains, and transmission power were incorporated as a function of power received in (3) below.

$$P_r = P_t + G_t + G_r - L_{FSPL} - L_{Atmospheric} \quad (3)$$

These three equations and models form the basis for the WPT analysis.

### 3.2 Orbital Optimization

The tradeoffs associated with the selection of an altitude, eccentricity, and inclination were compared in order to assess the economic merit of a certain orbital configuration. As a common basis for comparison, the tradeoffs associated with these parameters were converted to an economic factor via launch to low-Earth orbit costs for a SpaceX Falcon 9 launch vehicle (approx. \$2000/kg [10]). The cost-quantification process for orbital altitude, eccentricity, and inclination is presented below.

#### 3.2.1 Drag Modeling and Associated Costs

The main effects of altitude selection for any spacecraft are on atmospheric drag and the delta-v required for orbital insertion. The higher the altitude, the lower the drag and the higher the launch cost. The quantification of this tradeoff required the use of an

upper atmospheric density model of sufficiently high fidelity. For this purpose, the piecewise exponential model outlined in [14] was chosen for computational efficiency. The model presents an exponential relationship between atmospheric density and altitude with coefficients that vary in discrete altitude intervals. With density established as a function of altitude, the value of gas dynamic drag can be determined as per the familiar equation from continuum fluid dynamics below. Note that the coefficient of drag is a function of a myriad of parameters dependent on the geometry, surface finish, and thermodynamic properties of the surrounding medium [11]; this is, in part, due to the large mean free paths of the atmospheric particles, which undermine the validity of the continuum hypothesis by which the coefficient of drag is only a function of macroscopic parameters such as viscosity. A coefficient of drag of 2.0 was deemed suitable assuming a Z93 (a common spacecraft coating) wall finish and a thermal accommodation coefficient of 0.95.

$$D = -\frac{1}{2}\rho V^2 S C_D(\alpha, \beta, S, \sigma, T_w) \quad (4)$$

The relationship between drag and altitude can be translated to an engineering constraint on the spacecraft's propulsion system, given that higher amounts of thrust imply higher values of total impulse of the duration of the mission. Higher total impulse, for a specified thrust, implies the need for more propellant, which implies the need for stronger and more massive storage tanks, making the propulsion system as a whole more massive. The following constitutive equations along with the foregoing drag-altitude model are used to find the dependence of the propulsion system's mass on the altitude of the spacecraft. This analysis assumes Xenon as a propellant, which, although relatively costly, continues to be the most efficient propellant for electric thrusters. Given that Xenon and Argon can be stored at similar pressures as a compressed gas at room temperature, the analysis could be extended to cheaper gases such as Argon; however, the presented analysis with Xenon represents the most conservative estimate of the costs associated with drag-compensation and orbital station-keeping. Further, the following relations assume that the propellant of interest behaves like an ideal gas.

$$t = \frac{R_p P_G}{2 \sigma_{allow}} \quad (5)$$

$$R_p = \left(\frac{1}{4}V_G\right)^{1/3} \quad (6)$$

#### 3.2.2 Delta-V and Launch Costs

The delta-v required for orbital insertion to an orbit of specified altitude and eccentricity was calculated using standard Keplerian orbital mechanics and the relevant assumptions. The range of optimization for the altitude was 100 to 2000 km, while eccentricity was varied from 0 to 0.2. It is assumed that all orbital configurations are achieved by initial orbital insertion into a circular LEO of 100 km altitude and that the introduction of eccentricity into an orbit occurs instantaneously and during a single orbital maneuver from an initial circular orbit of radius equal to the radius at perigee of the desired final configuration. Thus, the relevant equation for the calculation of the required delta-v for a given altitude and eccentricity can be calculated by the application of **equation 7** to the orbital maneuvers of altitude increase and eccentricity change separately.

$$\Delta v = \sqrt{\left(\frac{2\mu}{r_i}\right) - \left(\frac{\mu}{r_f}\right)} \quad (7)$$

The resulting delta-v value is multiplied by a factor describing the cost per m/s of orbital velocity change. This allows for direct comparison of the launch costs and the costs associated with drag and wireless power attenuation. In the present project, the cost of a full payload delivery to low-Earth orbit by SpaceX's Falcon 9 launch vehicle was used as a first estimate; the corresponding cost is about \$5000 per m/s [10]. It is important to note that this cost is a sensitive function of the desired size of the space solar power satellite constellation. Most envisioned space solar power systems involve constellations of large sizes, so a single Falcon 9 launch vehicle would be insufficient for transportation, and the 'cost per delta-v' would increase.

### 3.2.3 Accounting for Orbital Perturbations: the J2 Effect

The oblateness of the Earth, along with the effects of atmospheric drag, constitute the highest order orbital perturbation terms for satellites in LEO. While the effect of drag was thoroughly accounted for in the Monte-Carlo simulation of spacecraft performance at varying altitude and eccentricities, the effect of the oblateness of the Earth requires complicated orbital calculations for rigorous accounting. For simplicity, only the first term (or the J2 term) is considered. The formula for the potential energy of an orbit accounting for the J2 term is presented below. Reference [12] shows that setting the inclination to certain critical values such as 63.4 deg or 116.6 deg. will minimize the secular drift of the orbit through its effect on the maximum value of the latitude. In particular, an inclination near 63.4 deg. will drive the precession of the argument of perigee to zero. This is economically

beneficial as it decreases the need for active control, simultaneously decreasing the complexity and weight of the space solar power system.

$$U = \frac{\mu}{r} + U_{J_2} + \dots \quad (8)$$

$$U_{J_2} = -\frac{3J_2\mu}{2r} \left(\frac{R_E}{r}\right)^2 \left(\sin^2(\varphi) - \frac{1}{3}\right) \quad (9)$$

For this reason, the desired inclination was set circa 63.4 deg. Out of all launch sites accessible to the United States, this would be most easily achievable by launching from the Pacific Spaceport Launch Complex in Kodiak, Alaska, located at a latitude of about 57.4 deg. After orbital insertion, the required delta-v for a pure inclination change to achieve the desired 63.4 deg would be about 800 m/s, using Keplerian dynamics. This is deemed economically favorable, as it is much lower than the overall delta-v required for orbital insertion to LEO, which is on the order of 10 km/s.

### 3.2.4 Repeating Ground Tracks and Altitude Selection

One of the major selling points of space-based solar power is its ability to provide access to solar energy regardless of local weather conditions. For this reason, early feasibility studies often focused on systems placed in geo-stationary orbit. Such an orbit would feature a continuous direct line of sight and potential for uninterrupted power transmission between the transmitting satellite and the ground station. However, the required altitude for a GEO is well outside the present range of analysis. This means that the satellite will inevitably shift in and out of sight of its designated ground station. To mitigate this effect, the orbit can be designed to have repeating ground tracks with a short repeat period. This, along with an adequately large constellation of solar power spacecraft at different points along the same ground-tracks, would facilitate the continuous coverage provided by GEO without its high launch costs.

The required orbital radius for repeating ground tracks is given below as a function of the number of spacecraft revolutions per rotations of the Earth.

$$a_{RGT} = \mu^{1/3} \left(\frac{M}{N\omega_E}\right)^{2/3} \quad (10)$$

Because repeating ground tracks are the only way to guarantee repeated coverage of a certain ground station for a space solar power station in LEO, their implementation is taken as a self-imposed mission

requirement. This will alter the ultimate ideal altitude as described in section 4.2.

### 3.2.5 Monte Carlo Analyses: Calculations

The foregoing cost quantification procedures for orbital insertion, drag-related constraints, and power attenuation were used to determine a total economic cost factor for 15,000 different configurations of altitude and eccentricity for spacecraft of the following frontal areas: 5 sq. m, 25 sq. m, and 125 sq. m. The results for 5 sq. m and 25 sq. m are given in section 4.

Furthermore, the probability distribution functions used in the space environment Monte Carlo are driven by the atmospheric observations given in **appendix C** [13], the results of which are outlined below in **figures 1 and 2**. Notice that the PDFs integrate to unity by definition.

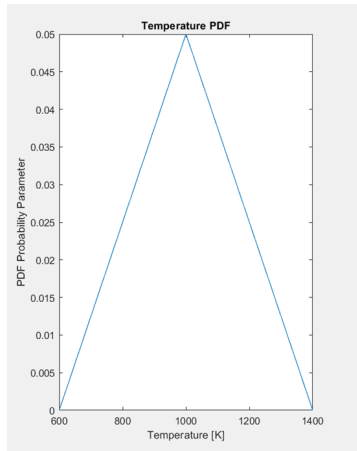


Figure 1

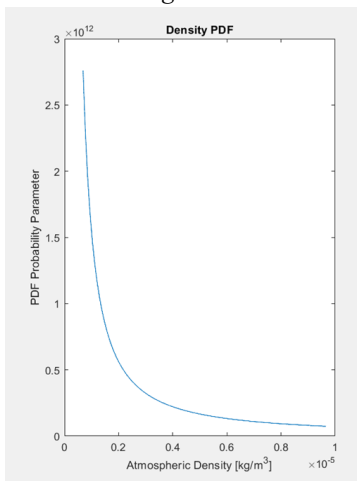


Figure 2

Discrete values in proportions driven by the distribution functions are then fed to the physical models driving drag and spacecraft wall heating. The

drag is calculated as per equation 4, while the model for spacecraft wall heating is given below [11].

$$T_w = \left( \frac{\rho u(u^2/(2+h))}{\epsilon \sigma} \right)^{1/4}$$

### 3.3 Propulsion System Selection

The propulsion system was selected by summing the total weights given by **Table 1** where each engine parameter has a value that corresponds to the grouping of each variable. The totals were summed as shown in **Appendix A** and the optimal engine is selected by being the highest valued selection compared to the entire array of engines considered. For specific variables within the analysis, the method of deriving a value was done by utilizing non-deterministic models such as the upper altitude density model [14] and utilizing drag models for free molecular flow as described in equation 4 [15].

The resultant thrust would be calculated from the general equation X, that is given the modeled drag and empirical thrust data.

$$T - D = T_{Resultant} \quad (11)$$

A logarithmic graph detailing the engines' optimal altitude can be found in **Appendix B**, where the domain of feasible operation for a given thruster is determined by the margin between its thrust and the gas-dynamic drag at a certain altitude.

## 4. Results and Discussion

In the following section, the results of the non-deterministic models will be shown and discussed.

### 4.1 Transmission Frequency Analysis

The first step in our analysis is to identify an optimal frequency for WPT. In order to identify this frequency, equation (3) was used, which takes into account FSPL (1), antenna gain (2), and atmospheric attenuation model using the ITU-R P.676-10 model.

Figure 3 below shows the FSPL as a function of Altitude in km from 100 to 2,000 km, which is the upper bound of LEO, and a Frequency of 0 to 100 GHz with the Attenuation plotted in dB.

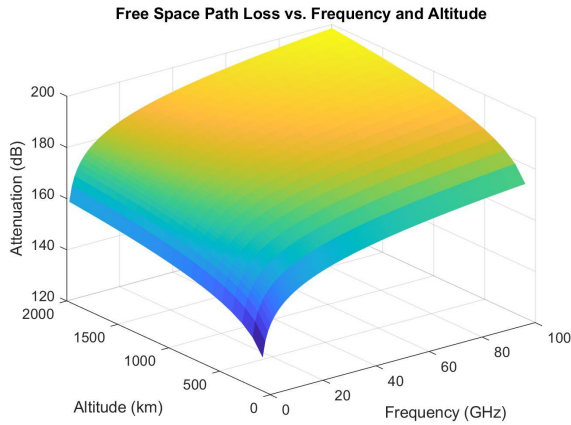


Figure 3

From Figure 3 above, it can be seen that there is an increase in attenuation as both altitude and frequency increase, with a logarithmic relationship between them.

Figure 4 below shows the atmosphere attenuation in decibels for a frequency of 0 to 100 GHz at an altitude of 100 km. Since atmospheric attenuation occurs in Earth's Atmosphere and not through space, this attenuation becomes a constant in our analysis once a frequency is identified. In order to calculate the atmospheric attenuation, a temperature of -52.6 C, an atmospheric pressure of 11394.46 Pa, and a water vapor density of .15 g/m<sup>3</sup> were used based on the atmospheric averages of these values between 0 and 100 km from [15]. Then, the ITU-R P.676-10 atmospheric attenuation model was applied [9].

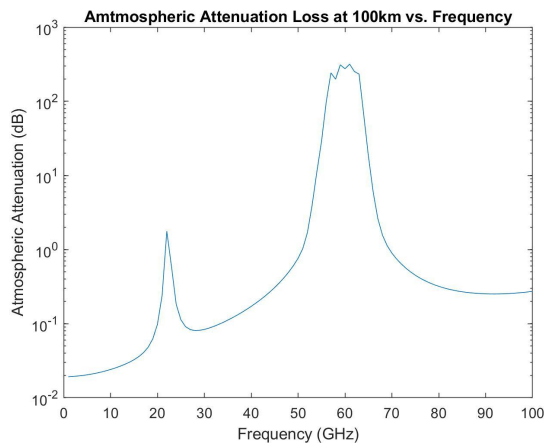


Figure 4

From Figure 4 above, it can be seen that there are two primary spikes in atmospheric attenuation losses which occur around 22 GHz and 60 GHz; these are due to water vapor and gaseous attenuation, respectively.

Below is Figure 5, which plots the power received and aperture area as a function of frequency. In order to calculate the power received, several

assumptions were made. First, a power transmission of 100 kW was assumed, which is a reasonable first estimate considering that the ISS produces around 90 kW of power [16]. Next, the transmitting antenna aperture area was assumed to be constant at 10m<sup>2</sup> while the receiving antenna, which is the ground station, varies from 0 to 100 km<sup>2</sup> in effective aperture area.

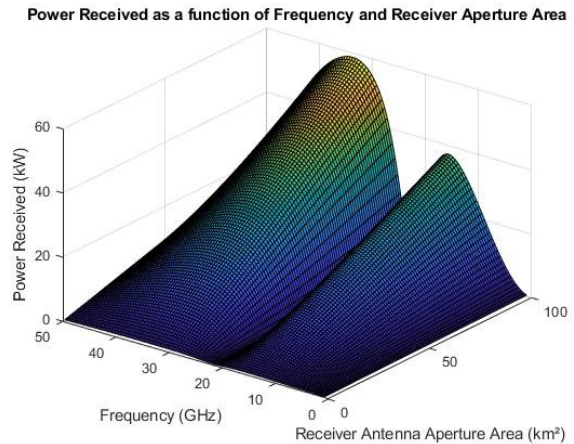


Figure 5

From Figure 5 above, it can be seen that there are two prominent peaks with a valley at ~20 GHz which is where water vapor effects in the atmosphere have the largest effects. Based on Figure 5, the peak occurs at 33.67 GHz, and the second peak occurs at a frequency of 15.78 GHz. Therefore, the optimal frequency to maximize power received would be 33.67 GHz, or if a lower frequency is needed due to technology readiness, safety, or regulatory constraints, then 15.78 GHz would be optimal. For the remainder of this analysis, a frequency of 33.67 GHz will be used.

Next, power loss is converted to an economic term as a function of orbital altitude. Several assumptions were required to be made in order to convert the power loss into an economic factor. The first assumption that was made is that the SPS will have an orbital lifetime of 50 years, which comes from heritage. The ISS will have an orbital lifetime of > 30 years, making the SPS orbital lifetime of 50 years not an unreasonable estimate [16]. The next assumption used is a price per kilowatt hour of \$0.23, which comes as a global average as calculated from [17] and can be seen in Appendix [D]. From these two assumptions, the power loss can be multiplied by the Time of Flight (ToF) and then multiplied by the price per Kilowatt hour. This economic loss term will then feed into our later analysis to identify the optimal altitude based on economic loss tradeoffs. Below is Figure 6, which plots the economic loss versus orbital altitude.

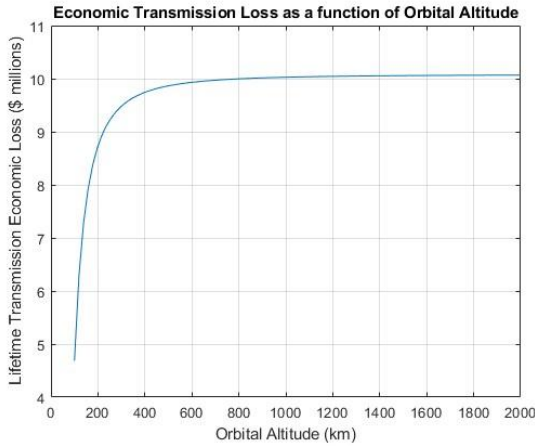


Figure 6

From Figure 6 above it can be seen that the economic loss due to power loss is between 8 and 18 million USD depending on orbital altitude and increases exponentially with orbital altitude.

#### 4.2 Orbital Configuration of Highest Economic Merit - Results of Orbital Monte Carlo

With the costs associated with gas dynamic drag, wireless power attenuation, and launch all in terms of a common economic basis, an estimated total economic cost, consisting of the sum of the three foregoing terms, was calculated for 15,000 different combinations of altitude and eccentricity. The results are presented graphically below in Figure 7 and Figure 8.

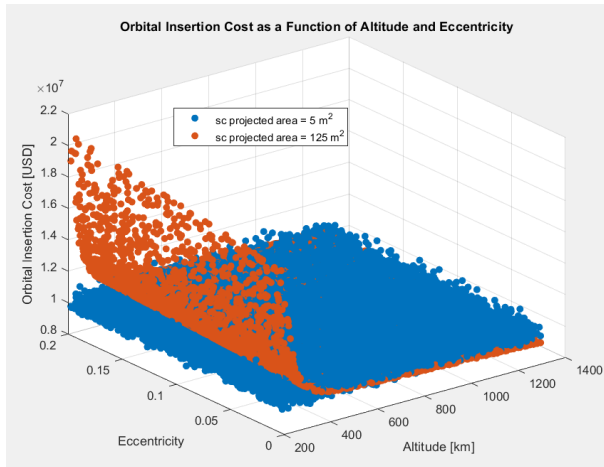


Figure 7

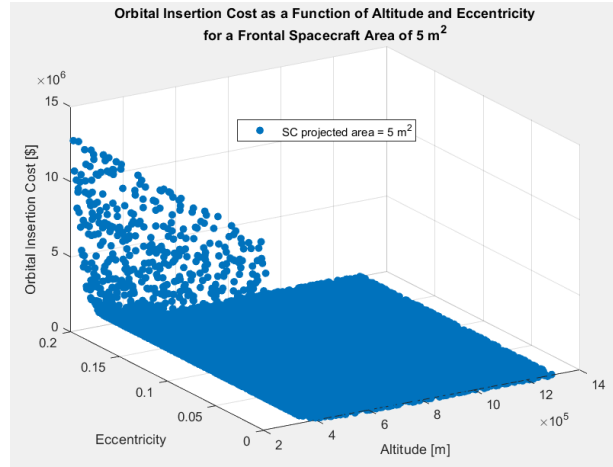


Figure 8

There is a notable exponential relationship between altitude and orbital insertion cost, as expected from the exponential relationship between drag-associated costs and altitude.

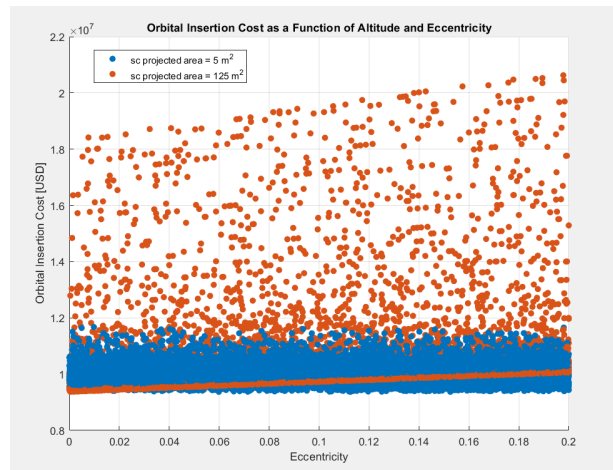


Figure 9

The foregoing 2D view of the multivariable optimization results in Figure 9 show a Pareto frontier that exhibits a linear relationship between eccentricity and economic cost. The higher the eccentricity, the higher the overall cost of the space-based solar power mission. This means that the optimal eccentricity tends to zero. The reason for this may be intuited from the fact that atmospheric drag tends to circularize orbits, so the design of a circular orbit eliminates the requirement of the propulsion system to control circularization. Furthermore, a circular orbit may simplify power transmission logistics by allowing the transmission spacecraft equal coverage of all points along its ground-tracks. The ideal altitude, eccentricity, and minimal relative economic cost (relative because it is not meant as an absolute economic measure but merely

for comparison between design alternatives) are given below in Table 2.

Table 2: Design alternatives given the spacecraft's projected area

Spacecraft Projected Area [m <sup>2</sup> ]	5	25	125
Optimal Orbital Altitude [km]	301	377	461
Optimal Eccentricity	-0	-0	-0
Total (Normalised) Economic Cost [USD*10E6]	9.38	9.73	9.94

The ideal orbital altitude increases significantly for solar power constellations of larger frontal area. The higher orbital altitude would drive launch costs up, especially for large architectures requiring multiple launch events. This indicates that the drag-associated cost term dominates the expression for economic cost, and constellations that minimize frontal area should be used to reduce mission costs.

The remainder of this section focuses on optimizing the orbital parameters for a constellation of 25 sq. m total frontal area as a case study. As mentioned in section, the self-imposed requirement for repeating ground tracks changes the ideal altitude from that presented in Table 2, which does not account for repeating ground tracks. The nearest altitude for repeating ground tracks to the ideal of 377 km for 25 sq. m frontal area is about 404 km, so this is taken as the optimal altitude for such a system. The ground tracks for a satellite at a circular orbit of 404 km altitude and 63.4 deg. inclination are given in Figure 10 below.

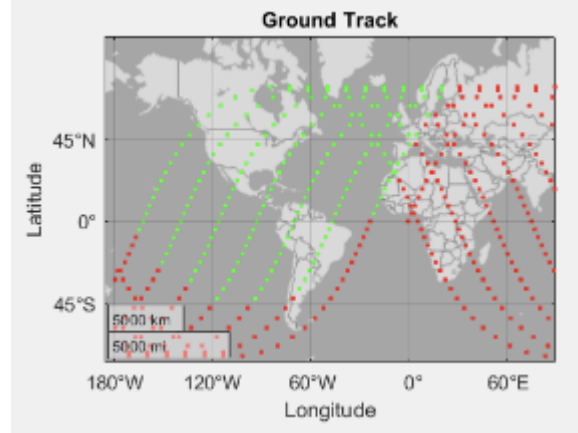


Figure 10

#### 4.3 Propulsion System Selection

Given that there is an optimal altitude of operation for an engine providing the maximum amount of thrust, it is suggested that for an altitude of ~400 km and inclination of ~63 degrees the MR-80B Throttling Rocket Assembly [18] is a favorable choice in terms of main engine use and MR-111C Rocket Engine Assembly Thruster [18] is a favorable thruster system to potential use for attitude control.

#### 5. Conclusions

This study aimed to assess the feasibility and economic merit of various design parameters for a solar power satellite (SPS) system. It considered various orbital configurations, transmission frequencies, and propulsion solutions. The results point towards higher economic efficiency for space solar power constellations that minimize frontal area, inspired by arrangements like SpaceX's Starlink. The optimal power transmission frequency for a 100 kW is approximately 33.67 GHz, which minimizes power loss due to atmospheric effects within the domain of analysis (0 to 50 GHz).

In the analysis of orbital configurations, the total economic cost function was found to vary non-monotonically with altitude. For low altitudes, marginally higher altitudes are more economically feasible due to the decrease in drag. However, for higher altitudes where drag becomes negligible, higher altitudes pose an increase in launch cost, which drives the ideal value down. For a constellation with a 25 sq. m frontal area, the ideal altitude is approximately 404 km, considering the need for repeating ground tracks. Further, the optimal eccentricity was found to be zero for all spacecraft frontal areas considered, likely due to the fact that atmospheric drag naturally circularizes orbits.

The propulsion system selection process involved a comprehensive trade study of various spacecraft engines, considering parameters like thrust-to-power ratio, altitude, thrust, specific impulse, and weight. Engine selection prioritized long-term operational considerations over initial launch costs.

This study contributes to the understanding of the economic feasibility of LEO Solar Power Satellites and highlights the importance of optimizing orbital parameters and propulsion systems for cost-effective space-based solar power generation.

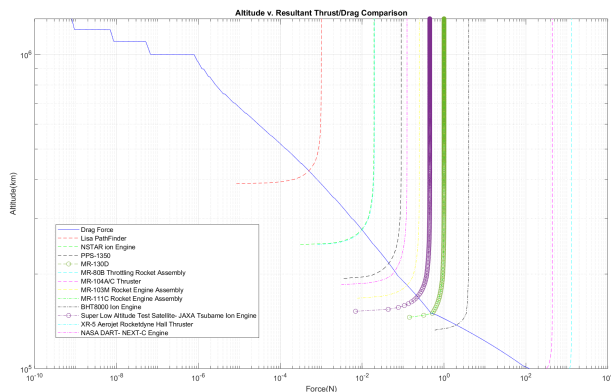
### Acknowledgments

The authors would like to acknowledge the assistance of Professor Adam Nokes and teaching assistants, Erika Hill, Aproova Tejaswi Karra, and Jad Bourjeili, in advising the Senior Capstone Project. The project would also have not been possible without the support of the following: the University of Texas at Austin: Aerospace Engineering & Engineering Mechanics Department, SPACE Canada and organizing officials, the International Astronautical Federation, the International Astronautical Congress, and its officials, class peers, and family and friends of all team members.

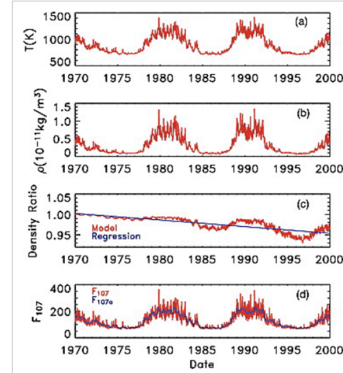
### Appendix A (Propulsion Decision Analysis)

Propulsion System	EP Ratio	Thrust (N)	Altitude (km)	Mass (kg)	Weight (kg)	EP Ratio	Thrust (N)	Altitude (km)	Mass (kg)	Weight (kg)	EP Ratio (2)	Thrust (2)	Altitude (2)	Mass (2)	Weight (2)
Space Shuttle Main Engine	1.65E-01	1.98E+05	424	10000	1	2	1	3	4	4	1	3	3	4	4
Space Shuttle External Tank	1.98E-01	1.09E+06	220	3000	4.2	2	3	3	2	2	0	0	0	3	4
Space Shuttle Solid Rocket Booster	0.02E-01	0.30	210	1000	0.55	3	2	3	2	2	1	0	0	3	4
Space Shuttle External Tank (Blue Assembly)	0.04E+01	2.04E	235	225	4.42	4	3	1	2	0	12	3	2	4	
Space Shuttle Solid Rocket Booster (Blue Assembly)	0.04E+01	140	275	230	1.46	1	4	3	1	1	9	12	3	2	4
Space Shuttle External Tank (White Assembly)	0.07E+01	1	215	224	5.30	1	2	3	1	4	2	6	3	2	4
Space Shuttle Solid Rocket Booster (White Assembly)	0.07E+01	1	247	221	0.16	1	2	3	1	4	2	6	3	2	4
Space Shuttle External Tank (Black Assembly)	0.20E+01	4	165	230	0.33	1	4	3	1	4	2	12	3	2	4
Space Shuttle Solid Rocket Booster (Black Assembly)	0.20E+01	0.444	168	210	20	1	3	3	1	2	9	3	4	2	
Space Shuttle External Tank (Black Assembly)	0.30E+01	0.32	162	200	40	1	2	3	1	1	2	6	3	2	2
Space Shuttle Solid Rocket Booster (Black Assembly)	0.30E+01	0.105	151	1167	12.3	1	2	3	1	1	2	6	3	2	2
Space Shuttle External Tank (Black Assembly)	0.30E+01	0.26	162	420	14	1	2	3	4	1	2	6	3	4	2

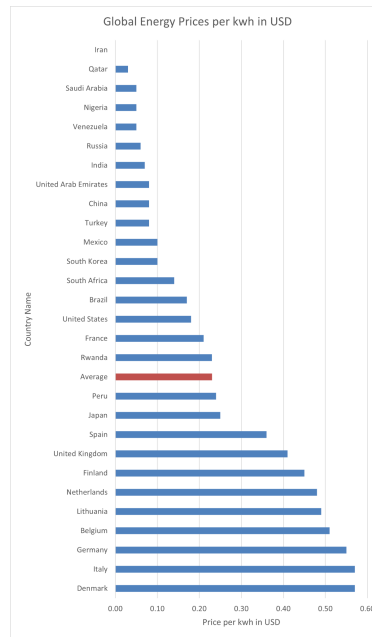
### Appendix B (Propulsion System Thrust vs Altitude)



### Appendix C (Fluctuations in Atmospheric Parameters Throughout Multiple Solar Cycles, [13])



### Appendix D (Global Energy Prices in USD per kwh)



### References

- [1] J.L. Canton, "Space-Based Solar Power: A Technical, Economic, and Operational Assessment", *U.S. Army War College*, [2015]. [Online]. Available: <https://press.armywarcollege.edu/cgi/viewcontent.cgi?article=1456&context=monographs>
- [2] Mani, A. and Chacko, O., "Attenuation of solar radiation in the atmosphere", in *Sun II (Conference Proceedings)*, 1979, vol. 3, pp. 2208–2212.

- [3] J. Mankins, "SPS-ALPHA: The First Practical Solar Power Satellite via Arbitrarily Large Phased Array (A 2011-2012 NASA NIAC Phase 1 Project)" *NASA* [Online]. Available: [https://www.nasa.gov/pdf/716070main\\_Mankins\\_2011\\_PhI\\_SPS\\_Alpha.pdf](https://www.nasa.gov/pdf/716070main_Mankins_2011_PhI_SPS_Alpha.pdf) [Accessed: 18-Feb-2023]
- [4] P. Jaffe, et. al., "Opportunities and Challenges for Space Solar for Remote Installations", *Naval Research Laboratory*, 2021. [Online]. Available: (PDF) "[Energy Orbit " Wirelessly Powering Satellites using Small Space Solar Power Satellite Constellation \(researchgate.net\)](#)"
- [5] W. C. Brown, "The history of wireless power transmission," *Solar Energy*, vol. 56, no. 1, pp. 3-21, 1996, [https://doi.org/10.1016/0038-092X\(95\)00080-B](https://doi.org/10.1016/0038-092X(95)00080-B).
- [6] C. T. Rodenbeck et al., "Terrestrial Microwave Power Beaming," in *IEEE Journal of Microwaves*, vol. 2, no. 1, pp. 28-43, Jan. 2022, doi: 10.1109/JMW.2021.3130765.
- [7] M. Tisaev, E. Ferrato, V. Giannetti, C. Paissoni, N. Baresi, A. Lucca Fabris, and T. Andreussi, "Air-breathing electric propulsion: Flight Envelope Identification and development of control for long-term orbital stability," *Acta Astronautica*, vol. 191, pp. 374–393, 2022.
- [8] K. Prathivadi et al., "Characterization of an Air-Breathing Deflagration Thruster", *AIAA, 2023 SciTech Forum*, [Online]. Available: [www.globalauthorid.com/WebPortal/ArticleView?wd=F2BEA4612AE1FD3D30622F9011C5FC9D7043808FBAF42088](http://www.globalauthorid.com/WebPortal/ArticleView?wd=F2BEA4612AE1FD3D30622F9011C5FC9D7043808FBAF42088). [Accessed: 03/15/2023].
- [9] Radiocommunication Sector of International Telecommunication Union. Recommendation ITU-R P.676-10: Attenuation by atmospheric gases 2013.
- [10] SpaceX, "Falcon 9 User's Guide," Massachusetts Institute of Technology, September 2021. [Online]. Available: <http://web.mit.edu/2.70/Reading%20Materials/SpaceX>
- [11] F. Hild, et al., "Optimisation of satellite geometries in Very Low Earth Orbits for drag minimisation and lifetime extension", *Elsevier*, vol. 201, pp. 340 - 352, December, 2022. [Online]. Available: <https://www.sciencedirect.com/science/article/abs/pii/S0094576522004970>. [Accessed Feb. 24th, 2023].
- [12] J. W. Wright, "Minimizing Secular J2 Perturbation Effects on Satellite Formations," M.S. thesis, Air Force Institute of Technology, March 2008.
- [13] H. Vickers, et al., "A solar cycle of upper thermosphere density observations from the EISCAT Svalbard Radar", *Journal of Geophysical Research: Space Physics*, vol. 119, no. 8, July, 2014. [Online]. Available: <https://agupubs.onlinelibrary.wiley.com/doi/full/10.1002/2014JA019885>
- [14] S. Kedare and S. Ulrich, "Design and Evaluation of a Semi-Empirical Piece-wise Exponential Atmospheric Density Model for CubeSat Applications", *AIAA 2015-1589*, January 2015. [Online]. Available: [Design and Evaluation of a Semi-Empirical Piece-wise Exponential Atmospheric Density Model for CubeSat Applications | AIAA SciTech Forum%20Falcon-users-guide-2021-09.pdf](#). [Accessed: 9/ 15/ 2023].
- [15] U.S. Standard Atmosphere, 1976. U.S. Government Printing Office, Washington, D.C.
- [16] Garcia, M. (2016, April 28). International Space Station Facts and Figures. NASA. <https://www.nasa.gov/feature/facts-and-figures>
- [17] Electricity prices by country 2022. Statista. (2023, August 29). <https://www.statista.com/statistics/263492/electricity-prices-in-selected-countries/>
- [18] "In-space data sheets 4.8 - Rocket," Aerojet Rocketdyne, <https://www.rocket.com/sites/default/files/documents/In-Space%20Data%20Sheets%204.8.20.pdf> (accessed Sep. 15, 2023).